Indian Journal of Research Foundation
An International Multidisciplinary Journal
www.indianjournal.net

RESEARCH ARTICLE

Synthesis and physicochemical characterization of rGO–Fe_3O_4 nanocomposite materials

G. Dharani, M. Vimala Joice *

PG and Research Center of Chemistry, Jayaraj Annapackiam College for Women (Autonomous), Periyakulam-625 601, Tamil Nadu, India

Received: 18 July 2026 / Revised: 22 September 2026/ Accepted: 1 October 2026
Corresponding author. E-mail: vjoiceche@annejac.ac.in*

ARTICLE INFO

Keywords

Nanocomposites
Graphene Oxide
Reduced graphene oxide
Ultrasonication
X-ray diffraction

ABSTRACT

Reduced graphene oxide (rGO)–Fe_3O_4 nanocomposites have attracted considerable attention due to their unique combination of electrical conductivity, large surface area, and magnetic properties. In the present study, rGO–Fe_3O_4 nanocomposites were synthesized through a simple chemical reduction and reflux-assisted approach. Reduced graphene oxide was prepared from graphene oxide using hydrazine hydrate as a reducing agent, while Fe_3O_4 nanoparticles were synthesized using ferric chloride, ferrous sulfate, and urea. The prepared Fe_3O_4 nanoparticles were subsequently incorporated onto rGO sheets to obtain the nanocomposite. Structural characterization was carried out using Fourier Transform Infrared (FT-IR) spectroscopy and X-ray Diffraction (XRD) analysis. FT-IR spectra confirmed the presence of Fe–O stretching vibrations characteristic of magnetite and indicated successful interaction between rGO and Fe_3O_4 nanoparticles. XRD patterns revealed the crystalline spinel structure of Fe_3O_4 and the characteristic diffraction peak of reduced graphene oxide, confirming successful nanocomposite formation. The results demonstrate that Fe_3O_4 nanoparticles were effectively anchored onto rGO sheets, resulting in improved structural stability and potential applicability in environmental catalysis, energy storage, and sensing applications.

Introduction

The rapid development of nanotechnology has stimulated extensive research into the design and fabrication of multifunctional nanocomposites with enhanced physicochemical properties for advanced technological applications. Among various carbon-based nanomaterials, graphene and its derivatives have attracted considerable attention due to their remarkable electrical conductivity, large specific surface area, excellent mechanical strength, and outstanding chemical stability [1–3]. Reduced graphene oxide (rGO), obtained by the chemical or thermal reduction of graphene oxide, retains many of the advantageous properties of pristine graphene while possessing residual oxygen-containing functional groups that facilitate the anchoring and uniform dispersion of nanoparticles on its surface [4,5]. These characteristics make rGO an excellent support material for the development of high-performance nanocomposites. Magnetic metal oxide nanoparticles have gained significant interest because of their unique magnetic, catalytic, and electronic properties. Among them, magnetite (Fe_3O_4) is one of the most widely studied iron oxide materials owing to its high saturation magnetization, low toxicity, biocompatibility, environmental friendliness, and excellent chemical stability [6,7].

Fe_3O_4 nanoparticles (NPs) exhibit remarkable redox activity and magnetic responsiveness, making them suitable for applications in catalysis, magnetic separation, environmental remediation, biomedical engineering, and energy storage systems. However, the practical utilization of pure Fe_3O_4 NPs is often limited by particle agglomeration resulting from strong magnetic interactions and their relatively low electrical conductivity, which can adversely affect their electrochemical performance [8].

To overcome these limitations, the incorporation of Fe_3O_4 NPs onto conductive carbon matrices has emerged as an effective strategy. In particular, rGO provides a highly conductive network that enhances

electron transport, prevents nanoparticle agglomeration, and increases the available surface area for electrochemical and catalytic reactions [9]. The strong interfacial interaction between Fe_3O_4 NPs and rGO sheets promotes efficient charge transfer and improves the structural stability of the composite material. Furthermore, the synergistic combination of magnetic Fe_3O_4 and conductive rGO results in improved electrochemical activity, enhanced adsorption capacity, and superior catalytic efficiency compared with the individual components.

Recently, rGO–Fe_3O_4 nanocomposites have been extensively investigated for a wide range of applications, including Li-ion batteries, supercapacitors, photocatalysis, wastewater treatment, magnetic separation, biosensors, and electromagnetic shielding materials. In energy storage devices, the high electrical conductivity of rGO facilitates rapid charge transport, while Fe_3O_4 contributes high theoretical capacity and redox activity, leading to improved energy storage performance. In environmental applications, the large surface area of rGO combined with the magnetic recoverability of Fe_3O_4 enables efficient adsorption and removal of organic pollutants and heavy metal ions from aqueous systems.

Moreover, the excellent biocompatibility and magnetic properties of Fe_3O_4-based nanocomposites have attracted considerable interest for biomedical applications such as targeted drug delivery, magnetic resonance imaging (MRI), and bio separation technologies [10]. The present study focuses on the synthesis of rGO–Fe_3O_4 nanocomposites through a simple chemical route and their characterization using Fourier Transform Infrared (FT-IR) spectroscopy and X-ray Diffraction (XRD) analysis.

The structural and functional characteristics of the synthesized nanocomposites were investigated to confirm the successful integration of Fe_3O_4 nanoparticles onto the rGO matrix. The resulting rGO–Fe_3O_4 nanocomposites are expected to exhibit enhanced electrical conductivity, magnetic responsiveness, and surface activity, making them promising candidates for applications in energy storage, environmental remediation, catalysis, corrosion-resistant coatings, electrochemical sensing, and biomedical technologies.

Experimental

Materials

Graphite powder, ferric chloride ($FeCl_3$), ferrous sulfate heptahydrate ($FeSO_4 \cdot 7H_2O$), urea (NH_2CONH_2), hydrazine hydrate, distilled water and ammonia solution were used without further purification.

Instruments

FT-IR and XRD analyses were employed for characterization. The infrared spectrum was acquired using a SHIMADZU FT-IR Affinity-1 spectrophotometer in the range of 400–4000 cm^{-1}, employing a KBr disc. Powder XRD was carried out using a Miniflex 600 DESKTOP X-ray Diffractometer.

.

Synthesis of reduced graphene oxide (rGO)

Graphene oxide (50 mg) was dispersed in 50 mL of distilled water and ultrasonicated for 1 h. Hydrazine hydrate was added as a reducing agent, and the mixture was heated at 90 °C for 90 min. The resulting black suspension was washed with distilled water and ammonia solution, centrifuged, and dried to obtain rGO powder [11].

Synthesis of Fe_3O_4 NPs

Ferric chloride, ferrous sulfate heptahydrate, and urea were dissolved in distilled water and heated under reflux at 90 °C for 6 h with continuous stirring. The precipitate obtained was filtered, washed, and dried to yield Fe_3O_4 NPs [12]. During the reaction, the solution gradually changed from a brownish colour to a black suspension, indicating the formation of Fe_3O_4 nanoparticles. The obtained precipitate was repeatedly washed with distilled water and ethanol to remove any residual impurities and unreacted precursors. The dried Fe_3O_4 NPs were finely ground and stored in airtight containers for subsequent characterization and composite synthesis.

Preparation of rGO-Fe_3O_4 Nanocomposite

Fifty milligrams of rGO was dispersed in distilled water by sonication. Fe_3O_4 NPs were added to the suspension, followed by hydrazine hydrate. The mixture was refluxed at 90 °C for 1 h under continuous stirring [13]. The resulting product was filtered, washed, and dried to obtain rGO–Fe_3O_4 nanocomposites. The synthesis pathway of the rGO– Fe_3O_4 nanocomposite is illustrated in Figure 1.

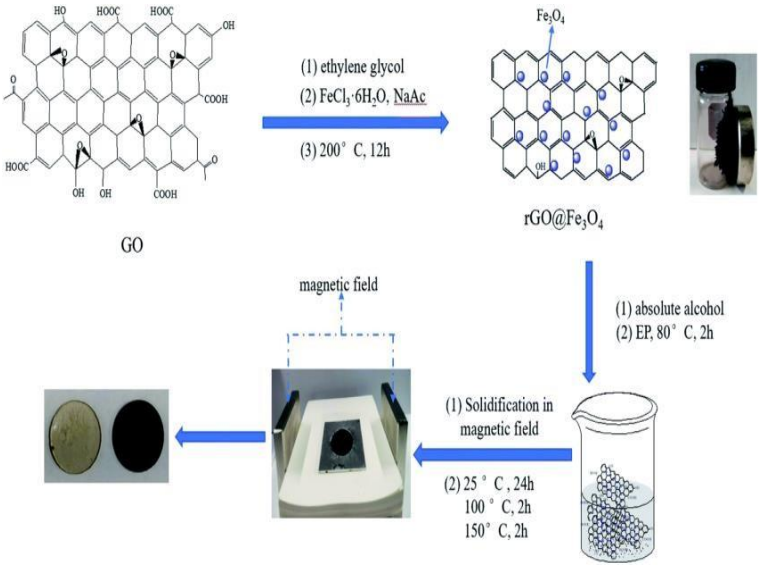


Figure 1. The synthetic pathway of the rGO–Fe_3O_4 nanocomposite.

Results and Discussion

FT-IR spectroscopy

The FT-IR spectra of the synthesized materials (Figure 2a,b) exhibit several characteristic absorption bands confirming the successful formation of the Fe_3O_4-based composite. A broad absorption band observed in the region of 3400–3200 cm^{-1} is attributed to O–H stretching vibrations of surface hydroxyl groups and physically adsorbed water molecules. The peaks located at 1607 and 1602 cm^{-1} correspond to the skeletal vibration of graphitic C=C bonds and the bending vibration of adsorbed water, indicating the presence of a carbonaceous framework. The absorption bands at 1035 and 1031 cm^{-1} are assigned to C–O stretching vibrations of residual oxygen-containing functional groups such as alkoxy and epoxy groups.

In Figure 2b, an additional peak at 1417 cm^{-1} is attributed to C–OH bending or carboxylate (COO^-) vibrations, suggesting the presence of oxygenated surface functionalities that can serve as anchoring sites for Fe_3O_4 Nps [14-17]. The characteristic bands at 531 and 533 cm^{-1} are assigned to Fe–O stretching vibrations, confirming the formation of magnetite (Fe_3O_4). The retention of oxygen-containing functional groups together with the Fe–O absorption bands demonstrate the successful incorporation of Fe_3O_4 NPs onto the graphene-based matrix and indicates strong interfacial interactions between the two components. A comparison of the FT-IR absorption bands of Fe_3O_4 NPs and the rGO–Fe_3O_4 nanocomposite is shown in Table 1.

Powder XRD

The XRD patterns of rGO and the rGO–Fe_3O_4 nanocomposite are shown in Figure 2c,d. The XRD pattern of rGO exhibits a broad diffraction peak centered around **2θ = 24–26°**, corresponding to the (002) plane of graphitic carbon. The broad nature of this peak indicates the largely amorphous structure of reduced graphene oxide and confirms the successful reduction of graphene oxide through the partial restoration of the sp^2 carbon network. The absence of the characteristic graphene oxide peak near 10–11° further suggests effective removal of oxygen-containing functional groups during the reduction process [18-20].

In the XRD pattern of the rGO–Fe_3O_4 nanocomposite, the broad diffraction peak associated with rGO is retained, indicating the presence of graphene sheets within the composite structure. The incorporation of Fe_3O_4 nanoparticles leads to changes in the diffraction profile and confirms the successful formation of the nanocomposite. The broad diffraction features and reduced peak intensity may be attributed to the nanoscale size of Fe_3O_4 particles and their homogeneous dispersion on the rGO surface. The absence of impurity peaks suggests the high purity of the synthesized material.

The interaction between Fe_3O_4 NPs and rGO sheets prevents the restacking of graphene layers and promotes the uniform distribution of magnetic nanoparticles throughout the carbon matrix. These results confirm the successful synthesis of the rGO–Fe_3O_4 nanocomposite and demonstrate the structural integration of Fe_3O_4 NPs with the reduced graphene oxide framework.

The rGO sheets provided a conductive support matrix and prevented nanoparticle aggregation, while Fe_3O_4 nanoparticles enhanced magnetic and redox properties. The synergistic interaction between rGO and Fe_3O_4 contributed to improved structural stability and increased surface area.

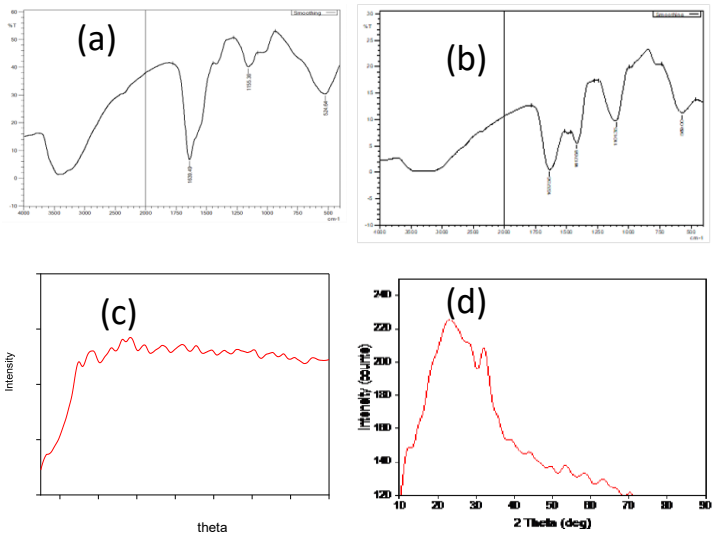


Figure 2 (a) FT-IR spectrum of synthesized Fe_3O_4 NPs**, (b)** FT-IR spectrum of the synthesized rGO–Fe_3O_4 nanocomposite, **(c)** XRD pattern of synthesized Fe_3O_4 NPs, and (d) XRD pattern of the synthesized rGO–Fe_3O_4 nanocomposite**.**

Table 1. FT-IR bands of Fe_3O_4 and rGO–Fe_3O_4 nanocomposite.

Nano-composite	ν(O–H)	ν(CO_2)	ν_b(H–O–H)	νs(C=C)	νs(C –O)	νs(Fe– O)
Fe_3O_4	~3400–3200	2347	1607	-	1035	531
rGO–Fe_3O_4	~3400–3200	2328	1602	1602	1031	533

Conclusion

The rGO–Fe_3O_4 nanocomposites were successfully synthesized through a simple chemical reduction and reflux-assisted method. FT-IR analysis confirmed the presence of characteristic Fe–O vibrations, while XRD analysis revealed the crystalline spinel structure of Fe_3O_4 along with the graphitic features of rGO. The successful incorporation of Fe_3O_4 NPs onto rGO sheets resulted in a stable nanocomposite with enhanced structural characteristics. Owing to the synergistic combination of conductivity, magnetic behavior, and large surface area, the synthesized material exhibits significant potential for applications in energy storage, environmental remediation, catalysis, and sensing technologies.

Acknowledgements

The authors express their sincere gratitude to the DST-FIST-supported Instrumentation Centre, Jayaraj Annapackiam College for Women (Autonomous), Periyakulam, for providing essential research facilities.

References

[1] M.D. Stoller, S. Park, Y. Zhu, J. An, R.S. Ruoff, *Nano Lett*., 8 (2008), 3498–3502.
[2] G. Williams, B. Seger, P. V. Kamat, *ACS Nano*, 2 (2008) 1487–1491.
[3] L. Qu, Y. Liu, J. B. Baek, L. Dai, *ACS Nano*, 4 (2010) 1321–1326.
[4] Y. Liang, H. Wang, J. Zhou, Y. Li, J. Wang, H. Dai, J. Am. Chem. Soc., 134 (2012) 3517– 3523.
[5] Z.S. Wu, W. Ren, L. Wen, L. Gao, J. Zhao, Z. Chen, G. Zhou, F. Li, H. M. Cheng, *ACS Nano*, 4 (2010) 3187–3194.
[6] K. S. Novoselov, A. K. Geim, S. V. Morozov, D. Jiang, Y. Zhang, S. V. Dubonos, I. V. Grigorieva, A. A. Firsov, *Science*, 306 (2004) 666–669.
[7] A. K. Geim, K. S. Novoselov, Nat. Mater., 6 (2007) 183–191.
[8] D. R. Dreyer, S. Park, C. W. Bielawski, R.S. Ruoff*, Chem. Soc. Rev*., 39 (2010) 228– 240.
[9] W.S. Hummers, R.E. Offeman, *J. Am. Chem. Soc*., 80 (1958) 1339.
[10] S. Sun, H. Zeng, *J. Am. Chem. Soc*., 124 (2002) 8204–8205.
[11] A.K. Gupta, M. Gupta, *Biomaterials,* 26 (2005) 3995–4021.
[12] M. Mahmoudi, S. Sant, B. Wang, S. Laurent, T. Sen, *Adv. Drug Deliv. Rev.,* 63 (2011) 24–46.
[13] C. Xu, X. Wang, J. Zhu, *J. Phys. Chem. C*, 112 (2008) 19841–19845.
[14] Y. Zhang, L. Zhang, C. Zhou, *Chem. Rev*., 113 (2013) 376–401.
[15] O.C. Compton, S.T. Nguyen, *Small,* 6 (2010) 711–723.
[16] H.P. Cong, X.C. Ren, P. Wang, S.H. Yu, *ACS Nano*, 6 (2012) 2693–2703.
[17] G. Wang, B. Wang, J. Park, J. Yang, X. Shen, J. Yao, *Carbon,* 47, (2009), 68-72.
[18] Y. Xu, K. Sheng, C. Li, G. Shi, *ACS Nano*, 4 (2010) 4324–4330.
[19] S. Bai, X. Shen, *Carbon*, 50 (2012) 2337–2346.
[20] X. Sun, C. Zheng, F. Zhang, Y. Yang, G. Wu, A. Yu, *Nanoscale Res. Lett*., 8 (2013) 1–9.